Fracture Mechanics of Concrete Structures
Proceedings FRAMCOS-3
AEDIFICATIO Publishers, D-79104 Freiburg, Germany

EXPERIMENTAL ANALYSIS OF RUPTURE MECHANISMS IN THE BRAZILIAN TEST

C. Rocco, G.V. Guinea, J. Planas, and M. Elices,
Departamento de Ciencia de Materiales, E.T.S.I. Caminos,
Universidad Politécnica de Madrid
Spain

Abstract
An experimental study was intended to clarify the mechanisms of rupture in the Brazilian test by considering the effects of specimen size and the width of the load bearing strip on the rupture process. The essential aspect of the methodology used in this research was that *stable tests* were performed, so that the sequence of cracking could be traced out. During the tests, the crack initiation and propagation were recorded. The results confirm the existence of *two fracture mechanisms* in the splitting test: one associated with the central cracks and the other with a secondary crack system on both sides of the bearing strips. The load-displacement curves recorded during the stable test show that *two peak loads* exist, one for each mechanism. The relative values of these peak loads depend on the specimen size and on the width of the bearing strip.
Keywords: Tensile strength, splitting test, size effect, rupture mechanisms, concrete.

1 Introduction

The splitting test, also known as the Brazilian test, is widely used to evaluate the tensile strength of concrete. Because of its simplicity, its use has extended to other materials such as rocks and ceramics. In this test, a cylindrical or prismatic specimen is compressed along two diametrically-opposed generators, as shown schematically in Fig. 1a. To prevent multiple cracking and crushing at the loading points, the load is distributed by two bearing strips, whose width veries according to the various standards. For relatively narrow strips, a nearly uniform tensile stress along the symmetrical plane of the specimen is achieved (Fig. 1b). Accordingly, the expected rupture mode is the split of the specimen in two across the plane of loading (Fig. 1c). The maximum (elastic) tensile stress value at failure gives a useful estimate of the tensile strength.

Although the rupture into two halves is the expected failure mode, other rupture modes have been observed. Hannant, Buckey and Croft (1973), Bazant, Kazemi, Hasegawa and Mazars (1991), and Castro Montero, Jia and Shah (1995), detected the development, in the Brazilian test of concrete and mortar specimens of several sizes, of diagonal cracks in the zone near the applied load. In these cases the specimens break through wedge formation and plastic slip, as sketched in Fig. 2a.

Other forms of rupture have been reported by Mitchel (1961), Colback (1966), Mooder (1979), Moseley, Ojdrovic and Petroski (1987), Ovri and Davies (1987) and Rudnik, Hunter and Holden (1988), in splitting tests performed with rocks, cement paste and ceramic materials in which the rupture is characterized by the development of a complex crack system, as shown in Fig. 2b.

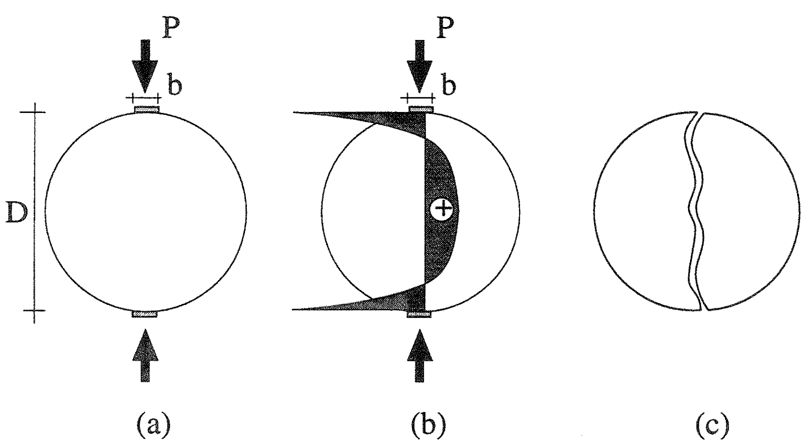

Fig. 1. Splitting test: (a) load configuration; (b) stress distribution and (c) rupture mode.

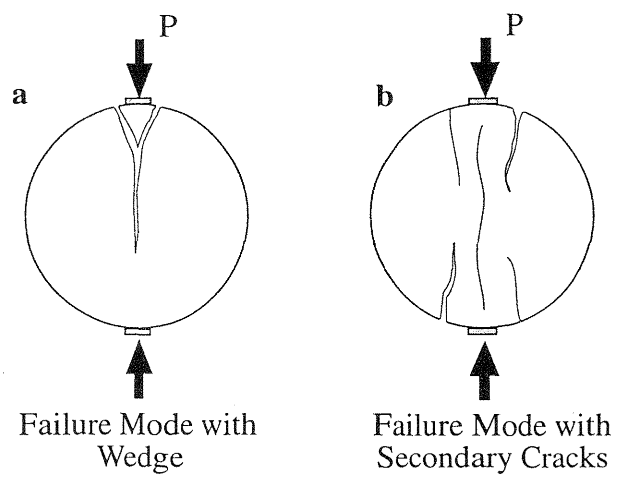

Fig. 2. Different rupture modes observed in the splitting test.

In recent years, the observation of modes of rupture different from the expected single-crack mode has raised doubts about the mechanisms of rupture in the Brazilian test, questioning the validity of the test itself as an appropriate method for estimating the tensile strength.

2 Experimental program

2.1 Mortar and granite specimens

Mortar prismatic specimens (series A) of square section were tested. The sizes of these specimens were: 17 mm, 38 mm, 75 mm, 150 mm and 300 mm, all of 50 mm thickness. The specimens were cut from pre-cast mortar plates of uniform thickness and were kept in water to prevent microcracking. The mortar used to cast the plates was of ordinary Portland cement (ASTM, Type I) and siliceous natural sand with a maximum aggregate size of 5 mm and a distribution within ASTM C33 limits. The water/cement and sand/cement ratios were 0.50 and 3.0 by weight, respectively. In addition, halved specimens were tested with the two halves assembled between the bearing strips so that the plane of contact between them coincided with the plane of loading.

Granite discs (series B) were tested, of 30 mm thickness and diameters 30 mm, 60 mm, 120 mm and 240 mm. The specimens were cut from granite plates of uniform thickness using cylindrical diamond drills. To eliminate any irregularity in the face cut, the specimens were ground.

2.2 Experimental set-up

Tests were conducted in a servo-hydraulic 1000 kN universal testing machine (Instron 1275). To control crack initiation and crack propagation, stable rupture tests were made. To obtain a stable loading sequence with crack propagation, the deformation along a diameter perpendicular to the load was controlled.

The bearing strips used to distribute the load were of 3 mm thick plywood. To study the effect of the width of the bearing strip, three different sets of strips were used, of widths 4%, 8% and 16% of the specimen size (b/D = 0.04, 0.08 and 0.16).

The growth of the crack traces in the faces of the mortar specimen was continuously video-recorded throughout the rupture process, and the images were fed to an image processing system for digital analysis.

3 Experimental results

3.1 Rupture process

Both samples, mortar and granite, showed the same rupture process, summarized in Fig. 3: the crack starts at the center of the specimen (A), and propagates toward the loading strips (B). Once the central crack has extended along the plane of symmetry of the specimen, secondary cracks appear at the edges of the specimen, arranged symmetrically at both sides of the bearing strips (C). These cracks grow deeper into the specimen,

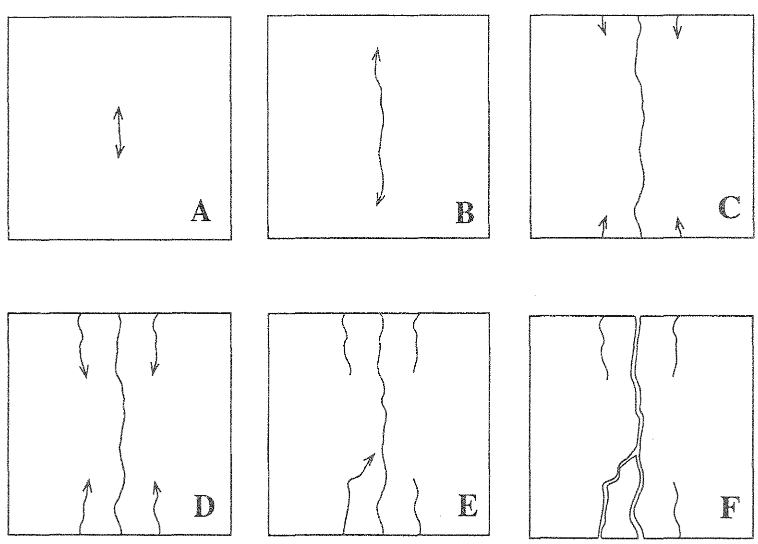

Fig. 3. Sequence of the crack propagation during the splitting test.

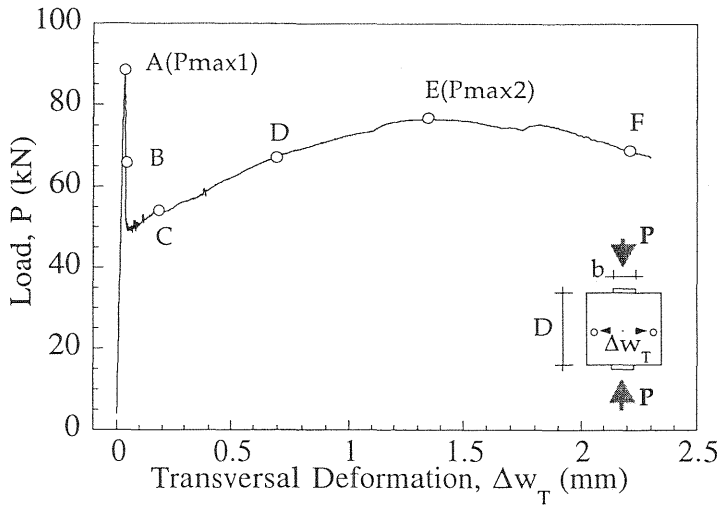

Fig. 4. Load-deformation curve of the stable splitting test in a mortar specimen (D = 300 mm and b/D = 0.16). The points correspond to the images in Fig. 3.

approximately parallel to the central or principal crack (D and E). In the final part of the test, the secondary crack growth becomes assymmetric until an unstable configuration is reached, usually followed by formation of a mechanism (F).

The curve of load vs. transversal deformation for the same test is shown in Fig. 4. The points corresponding to the different sketches in Fig. 3 are indicated on the curve by open circles labeled with the same letters. The curve presents two peak loads (points A and E). The first peak coincides with the initiation of the crack in the central zone of the specimen (point A). The unloading immediately after this peak load corresponds to the extension of the principal crack (point B). When the principal crack approaches the bearing strips, the unloading stops and the load increases again. During this reloading, the secondary cracks appear and grow symmetrically (points C and D). This continues until one of the secondary cracks begins to extend further, reaching the second peak of load (point E); then the load decreases while the secondary crack continues opening (point F). This secondary crack opening proceeds until the total fragmentation of the specimen.

In conclusion, two kinds of cracks occur during the test: the principal crack starts at the centre of the specimen and extends across the loading plane. The secondary system appears later at the edges of the specimen and grows symmetrically inwards, parallel to the main crack. Similar cracking processes were observed in tests with other specimen sizes, and other load-bearing strip widths. They were similar in the tests on granite discs.

3.2 Effects of specimen size and width of bearing strips

The curves of load versus transversal deformation (P-Δw_T) for granite and mortar specimens during stable splitting tests are similar.

Fig. 5 shows the corresponding curves for granite; the curves are for *different specimen sizes* (30 mm, 60 mm, 120 mm and 240 mm) and the *same relative width of the bearing strips* (b/D = 0.16, as recommended in the ASTM C496 standard). Each curve represents the average of four (4) tests.

To facilitate the comparison, the curves are drawn relative to the values of the load and the transversal deformation at the first peak load (P_{max1}). Note that in relative terms, the maximum load associated with the mechanism governing secondary crack propagation increases as the specimen size decreases. So in small specimens, the peak load associated with the secondary crack system can become the dominant peak load.

Fig. 6 shows the curve of load versus transversal deformation (P-Δw_T) for mortar specimens during the stable splitting test for specimens of the *same size* (D = 150 mm) and *different relative width of bearing strips* (b/D = 0.04, 0.08 and 0.16). It is seen that the width of the bearing strip only affects the part of the curve associated with the secondary cracking mechanism. As the width of the bearing strip decreases, the load that can be supported by the specimen during the

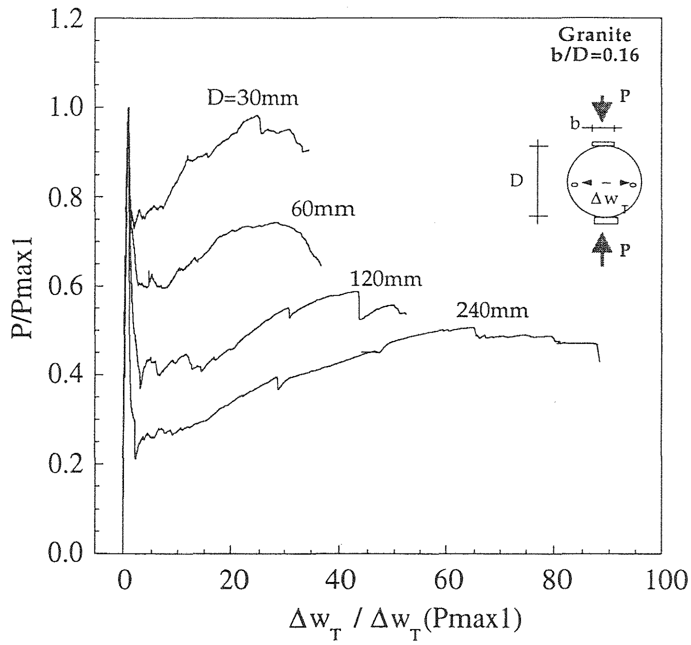

Fig. 5. Size effect in the curves load versus transverse deformation. Granite specimens tested with the same relative width of bearing strip (b/D = 0.16).

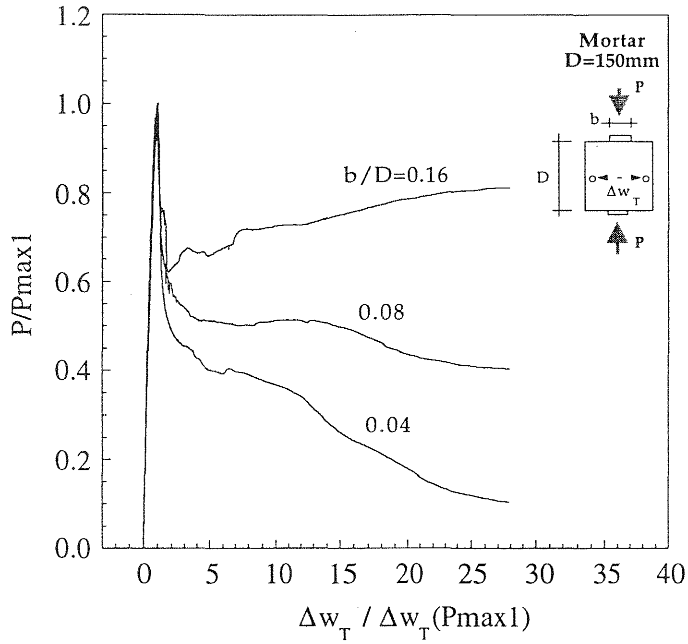

Fig. 6. Effect of width of bearing strips on the curves load versus transverse deformation. Mortar specimens of equal size (D = 150 mm).

propagation of the secondary cracks decreases significantly and eventually disappears for small enough widths of the bearing strips.

The curves show that the P-Δw_T behaviour during the secondary cracking is very sensitive to the size and to the width of the bearing strip but the softening branch associated with the growth of the principal crack is not affected by the width of the bearing strip.

4 Rupture mechanisms

From the experimental results, the following rupture mechanism emerges:

In the first stage, or *principal rupture mechanism*, the splitting test is governed by the maximum tensile stresses along the loading diameter of the specimen. These stresses control both the central crack localization and the propagation from the centre of the specimen to the edges. As seen in the propagation sequence in Fig. 3, during the initiation of this crack, a maximum load value is reached (P_{max1}). Then the specimen is unloaded as the crack extends to the edges. According to the standard test method, this maximum load value has to be used to evaluate the tensile strength in the splitting test.

In a second stage, the final or *secondary rupture mechanism* is operative. When the principal crack extends, the specimen is split into two pieces linked by the bearing strips as illustrated in Fig. 3C. Therefore, after the main crack growth, the specimen is reduced to two halves, each resisting the load applied across the bearing strips.

In accordance with this new mechanism, although the principal crack splits the specimen in two parts, the specimen is loaded until the halves break down and a new rupture load or peak load appears.

An analysis was made of the stress state in the specimen with this new load configuration using a finite element method. The results show that the maximum tensile stress occurs at the edges of the specimen near the end of the bearing strip. The location of the points of maximun tensile stress in the half specimen coincides very approximately with that of the secondary cracks recorded during the tests.

The most important consequence of the existence of the two mechanisms is that two peak loads exist, one associated with each mechanism. As seen in Figs. 5 and 6, the relation between the peak loads of each mechanism depends principally on the specimen size and the width of the bearing strips. When this width is small, the second peak decreases or even disappears. However, for a relative width of 16%, as recommended in the ASTM C496 standard, the second peak can be higher than the first.

In a standard test, where the $P\text{-}\Delta w_T$ is not recorded, only the overall maximum load is recorded. Therefore, to determine accurately the tensile strength, it is important to ensure that the maximum load thus measured corresponds to the first peak. If this condition is not met, the splitting test is not valid.

To simulate experimentally the *secondary rupture mechanism*, specimens were cut in two halves and tested with the cut plane simulating a smooth principal crack between the bearing strips. The test conditions were similar to those used with standard specimens.

The localization and form of crack propagation during the half specimen test were similar to those observed in the secondary cracks in the whole specimen test. This confirms the validity of the secondary rupture mechanism proposed for the test.

The most important difference between the rupture of the cut halves and that of whole specimens is the wedge slip observed in the cut halves, where the central crack is simulated by one ideal smooth crack dividing both the specimen and the applied load into two exactly equal parts that impose one strong symmetry condition on the secondary crack growth. This enforced symmetry means that no preferential growth is possible and the rupture is produced through an additional rupture mechanism consisting in slip-wedge formation. This does not occur in the ordinary specimen test (entire specimens) because the meandering central crack breaks the symmetry condition and the rupture is governed by the asymmetrical growth of a secondary crack, which occurs before the wedge slip can form.

5 Final comments

Stable splitting tests disclose the mechanical behaviour and the cracking sequence of the specimen in the splitting test. The test results show that specimen rupture occurs through two mechanisms called *principal* and *secondary* mechanisms. The *principal mechanism* is associated with the main crack growth from the center of the specimen toward the bearing strips. This mechanism is governed by the maximum tensile stress normal to the loading plane. The *secondary mechanism* occurs after the principal crack has extended; secondary cracks appear at the edges of the specimens at both sides of the bearing strips and grow inwards parallel to the principal crack. The experiments showed that the cracking sequence during the splitting test depends neither on the size of the specimen nor on the width of the bearing strip.

Of central importance is that each of these mechanisms has an associated maximum load, so two peak loads may occur during the test. The experiments show that the relative values of the two peak loads depend on the specimen size and on the width of the bearing strip. When the specimen size decreases and the width of the bearing strip increases, the maximum load supported by the specimen during the secondary mechanism (during the secondary crack propagation) comes close to the maximum load associated with the principal mechanism. The secondary peak can become dominant, i.e. be the larger, for small specimens and wider bearing strips. This phenomen is important because in a standard test only the maximum of the two peak loads is recorded. This means that it is necesary to use specimen sizes and widths of bearing strips which guarantee that the maximum load in the test corresponds to the principal mechanism. Otherwise the splitting test is not valid.

6 Acknowledgments

The authors gratefully acknowledge support for this research provided by CICYT, Spain, under grants MAT97-1007-C02-2 and MAT97-1022. Also, to the Ministry of Education and Science, Spain, for the collaboration given by the Foreign Scientifics Program.

7 References

Bazant, Z., Kazemi, M., Hasegawa, T. and Mazars, J. (1991) Size effect in Brazilian split-cylinder test. **ACI Materials Journal**, 88(3), 325-332.

Castro Montero, A., Jia, Z. and Shah, S. (1995) Evaluation of damage in Brazilian test using holographic interferometry. **ACI Materials Journal**, 2, 268-275.

Colback, P. (1966) In **Proceedings of the First Congress of the International Society of Rock Mechanics**, Lisbon.

Hannant, D., Buckey, K. and Croft, J. (1973) Effect of aggregate interlock size on the use of the cylinder splitting test as a measure of tensile strength. **Materials and Structures**, 6, 15-21.

Mitchel, N. (1961) The indirect tension test for concrete. **Materials Research & Standards**, 1, 780-788.

Modeér, M. (1979) A fracture mechanics approach to failure analysis of concrete materials. **Report TVBM-1001**, Division of Building Materials, University of Lund.

Ojdrovic, R. and Petroski, H. (1987) Fracture behavior of notched concrete cylinder. **Journal of Engineering Mechanics, ASCE**, 113,10, 1551-1564.

Ovri, J. and Davies, T. (1987) Diametral compression of silicon nitride. **Materials Science and Engineering**, 96, 109-116.

Rudnik, A., Hunter, A. and Holden, F. (1988) **Materials Research & Standards**, 3, 283-289.